ISSN 0915-633X

NATIONAL INSTITUTE FOR FUSION SCIENCE

Experiments of an Intense H^- Ion Beam Acceleration

A. Ando, Y. Takeiri, O. Kaneko, Y. Oka, K. Tsumori, E. Asano,
T. Kawamoto, R. Akiyama and T. Kuroda

(Received - July 25, 1995)

NIFS-369 Aug. 1995

RESEARCH REPORT
NIFS Series

This report was prepared as a preprint of work performed as a collaboration research of the National Institute for Fusion Science (NIFS) of Japan. This document is intended for information only and for future publication in a journal after some rearrangements of its contents.

Inquiries about copyright and reproduction should be addressed to the Research Information Center, National Institute for Fusion Science, Nagoya 464-01, Japan.

NAGOYA, JAPAN

Experiments of an intense H^- ion beam acceleration

A.Ando [a], Y.Takeiri, O.Kaneko, Y.Oka, K.Tsumori,
E.Asano, T.Kawamoto, R.Akiyama and T.Kuroda

National Institute for Fusion Science, Nagoya 464-01, Japan

abstract

An intense H^- beam of a single beamlet is extracted from a large multicusp plasma source operated with cesium seeding. The H^- beams are accelerated up to 100keV by a single-stage or a two-stage electrode system. Spatial profiles of the beams are measured calorimetrically and a minimum beam divergence angle of 5mrad is achieved at a H^- current density of 30mA/cm^2 with a beam energy of 100keV. A ratio of an acceleration current to a H^- current increases abruptly when a H^- current saturates in the space charge limited region. This enhancement is mainly due to secondary electrons caused by the intersection of H^- beams with an extraction grid. When an operating gas pressure decreases, the ratio of the acceleration current to the H^- current decreases. This is related to a stripping loss of H^- ions in the electrodes. A beam divergence angle becomes minimum when a ratio of V_{acc} to V_{ext} is set at a optimum value of 1.6 in the single-stage acceleration. This ratio is almost the same as that in the double-stage acceleration, where the optimum ratio of E_{acc1}/E_{ext} is 1.5. In the optimum E_{acc1}/E_{ext} ratio the divergence angle is not affected by V_{acc2}. The divergence angle can be reduced by changing V_{acc2} even if the ratio of E_{acc1}/E_{ext} is not optimized. The beam steering effect by permanent magnets buried in an extraction grid is observed in nine beamlets experiments. A simple calculation of a single particle trajectory gives a good approximation of the beam deflection angle.

Keywords : Negative hydrogen ion source, NBI, High current density, Beam divergence, Beam deflection, Beam intersection with grids, Stripping loss of H^-.

1. Introduction

In the nuclear fusion research, the neutral beam injection (NBI) is one of the most promising methods for a plasma heating and/or a current drive and has been utilized in many plasma confinement devices. A scale of plasma devices becomes large and a beam energy more than 100keV is required in the next stage of NBI system. Since a neutralization efficiency is low in positive ions in the energy range, the negative-ion-based NBI system is required. Therefore, it is necessary to investigate production and acceleration characteristics of H^-/D^- ion beams and to develop large current negative ion sources. The ITER (International Thermonuclear Experimental Reactor) - NBI system is required to inject the D^- beam power of 50MW with an injection energy of 1.0MeV.[1]

In the development of the negative ion sources, a few amperes of H^- ions were extracted from multicusp sources in pure hydrogen discharges.[2-4] Recently, it was reported that an enhancement of the H^- ion current is induced by seeding a small amount of cesium (Cs) vapor into a multicusp plasma source.[5-7] A H^- current up to 10A has been obtained in the Cs-seeded sources.[8-11]

In the LHD (Large Helical Device) project, conducted by National Institute for Fusion Science, the negative-ion-based NBI system (total injection power : 20MW, injection energy : 125keV for hydrogen, 250keV for deuterium) has been proposed.[12] The ion source is required to deliver 45A of H^- ion current from an extraction area of 25 x 150 cm^2. The LHD has super-conducting helical coils to generate a magnetic field for the plasma confinement. Since the device is surrounded by a large cryostat for thermal insulation, it has small-sized injection ports for NBI. It is necessary to obtain a H^- ion beam with a high current density of 30 mA/cm^2 and with a low beam divergence of 0.5deg (9mrad) to inject the full beam power into the device.

In the research and development we have fabricated 1/6 and 1/3-scaled sources and successfully obtained a H^- ion beam of 16A with a current density of 45 mA/cm^2.[13] The arc efficiency (the ratio of H^- current to input arc power) was improved up to 0.1A/kW and H^- beams above 10A were accelerated up to 125keV.[14,15] It is one of key issues in the R&D to confirm the low beam divergence of H^- ion beam at a high current density.

It has been demonstrated at JAERI (Japan Atomic Energy Research Institute) that the H^- ion beams are accelerated up to 400keV with the current density of 13mA/cm^2 and the beam divergence angle of 5mrad.[16] Since an ion beam is considered to diverge with increasing the current density by the space charge effect, it should be demonstrated experimentally to accelerate high current density H^- ions with a low beam divergence angle.

It is also important to suppress electrons accelerated with negative ions in the high energy acceleration of negative ion beams. As a ratio of an acceleration current to a H^- current becomes large, a larger power supply system is required and heat load to each grid becomes large. An electric breakdown in the acceleration gap may be enhanced by the accelerated electrons. Electrons extracted with H^- ions are bent by a magnetic field due to permanent magnets buried in the extraction grid and can not penetrate into the acceleration gap. It is considered that the electrons accelerated in the acceleration gap are generated by the following two processes; one is a stripping process of H^- ions in the gap and the other is a secondary electron emission due to collisions of H^- ions with grids. The ratio of an acceleration current to a H^- current should be investigated in conjunction with an operating gas pressure and beam optics.

In this paper, we describe experimental results of a H^- beam acceleration from a single beamlet or nine beamlets. H^- beams are accelerated up to 100keV with a current density of 30mA/cm^2. A divergence angle is determined from a measured beam profile and a dependence of the divergence angle on an acceleration voltage is obtained. The ratio of an acceleration current to a H^- current is measured in various conditions of a pressure, an input arc power, an extraction voltage and an acceleration voltage. Experiments in a single-stage and a double-stage acceleration electrode systems are compared with each other.

The beam steering effect by the permanent magnets buried in the extraction grid was pointed out in a 49-holes experiment in JAERI.[17] This effect is a crucial problem to focus ion beams from multi-beamlets. We have also confirmed this effect by operating with 9 beamlets extraction system and compared the shift with calculation results.

2. Experimental Apparatus

A schematic view of the negative ion source is shown in Fig.1. This source is a 1/3-scaled one for the LHD-NBI source. The size of a rectangular multicusp plasma source chamber is 37cm in width, 62.5cm in height and 18.5cm in depth. An arc plasma is produced by using 18 tungsten filaments of 1.8mm in diameter attached on the chamber wall. This source is the same one from which 16A of H^- current was obtained.[13] Several modifications are made in the source to improve an arc efficiency. The magnetic filter which reduces electron density and temperature near the extraction apertures has been changed from a rod-type one (10mm in diameter) to a rectangular bar-type one (14 x 24 mm^2) in order to improve a transparency and an arc efficiency. Four bar-type magnetic filters with water cooling channels are installed in front of the plasma grid. Each bar is separated by 208mm and the magnetic field strength between the filters is 55G. A molybdenum liner is attached on the chamber inner wall to avoid Cs condensation on the wall. The separation between the liner and the wall is reduced from 5mm to 2mm, resulting in an increase of a cusp field strength from 0.8kG to 1.0kG. The size and structure of the filaments are also modified.

A single beam experiment is done with a single-stage and a double-stage beam acceleration electrode system as shown in Fig.2(a),(b), respectively. A plasma grid facing an arc plasma is made of molybdenum without water cooling. The other grids are made of oxygen-free copper. Permanent magnet arrays are buried in an extraction grid to deflect electrons extracted together with negative ions. An acceleration and a grounded grid are set in the double-stage acceleration and only a grounded grid is set in the single-stage acceleration. An extraction voltage V_{ext} is applied between the plasma grid and the extraction grid up to 9.5kV, a first acceleration voltage V_{acc1} is applied between the extraction grid and the acceleration grid up to 40kV, and a second acceleration voltage V_{acc2} is applied between the acceleration grid and the grounded grid up to 90kV. In the single-stage experiment, an acceleration voltage V_{acc} is applied between the extraction grid and the ground grid up to 90kV.

A multi-hole experiment is also done with the double-stage acceleration system. Nine holes of 13mm in diameter is arranged in an area of 5 × 5cm^2. The beam pulse length is kept at 0.3 sec during the experiments.

In order to seed Cs vapor into the source chamber, a Cs oven are attached on an end plate of the chamber through a valve. The oven can be heated up to 300 ℃. Guiding tubes and the valve are heated at higher temperature than that of the oven to prevent cesium condensation. An amount of Cs vapor is controlled by changing a duration of the valve opening and an oven temperature. In the experiment the oven temperature is kept relatively low and Cs vapor is slowly seeded in the source. When the Cs effect, such as an enhancement of a H^- current and a decrease of an extraction current, appears during the operation, the valve is closed and no more Cs is supplied afterward. A total amount of Cs is estimated to be less than 100mg. The plasma grid temperature is important for the Cs-seeded operation. The grid is heated by radiation from filaments and particle influx from arc discharges. Its temperature is monitored by a thermo-couple and is around 300 deg during the experiments.

The total H^- ion currents are measured with a two-dimensional (2D) calorimeter array, which has a cross shape and spatial beam profiles in both horizontal and vertical directions are measured simultaneously in a shot. There are 19ch calorimeters in the horizontal and also 19ch ones in the vertical direction. The current density at each point is calculated from temperature rise of the calorimeter. The total H^- ion current is obtained from the profiles. The array can be moved in the vertical direction and the whole 2-D spatial profile can be obtained. Permanent magnets are placed in front of each calorimeter to remove accelerated electrons. This array is placed at 2.0m downstream from the plasma grid in the experiments. The total H^- ion current and the current density mentioned in this paper are the values at the calorimeter.

3. Experimental results and Discussion

A. Characteristics of the H^- beams extracted from the source

Several characteristics of the H^- beams are investigated in a single beamlet and the single-stage acceleration electrode system. Here, the extraction gap, d_{ext}, and the acceleration gap, d_{acc}, are set at 4.5mm and 40mm, respectively. A dependence of a H^- current on an input arc power P_{arc} is measured and is shown in Fig.3(a). The arc power is determined by the product of an arc current, I_{arc}, and an arc voltage, V_{arc}. The extraction voltage V_{ext} is set at three different values. When V_{ext} is fixed, the H^- current increases linearly with P_{arc}, corresponding

to the plasma density limited operation, where the H^- current is proportional to the plasma density. As P_{arc} increases more, the H^- current saturates. This saturation corresponds to the space charge limited operation. In the figure the arc powers where the saturation occurs are indicated by arrows. When V_{ext} increases, the H^- current increases again. These characteristics has been also observed in the multi-hole experiments.[10,11,13,14] An extraction current, I_{ext}, increases almost linearly with P_{arc} and the ratio of I_{ext}/H^- is lower than 2.

In Fig.3(b) the acceleration currents I_{acc} are also plotted to P_{arc}. There observed a sudden increase in I_{acc} at the P_{arc} where the H^- current saturates. The ratio of I_{acc} to H^- current, I_{acc}/H^-, is also plotted in Fig.3(c). The ratio is kept constant at 1.3-1.5 before the saturation and increases abruptly when the saturation occurs. It is considered that the sudden increase of the acceleration current is due to the secondary electrons emitted from the extraction grid by collisions of diverging H^- ions with the grid. In the space charge limited region where the H^- current saturates, the H^- emission surface is distorted and the beams tend to diverge. The expanded beams collide with the extraction grid and the emitted secondary electrons are accelerated. Though the magnetic field by the permanent magnets is also present in the acceleration gap, it seems to be insufficient for the suppression of the secondary electrons.

The constant ratio of I_{acc}/H^- before the saturation in Fig.3 is related with the filling gas pressure, p. Figure 4(a) shows the dependence of H^- current and I_{acc} on p. The maximum H^- current is obtained at p = 0.7Pa. As the pressure decreases, the difference between H^- current and I_{acc} becomes small and the ratio gets close to 1. Figure 4(b) shows the ratio of I_{acc}/H^- as a function of p. The ratio becomes large as the pressure increases. This indicates that the ratio is determined by the stripping loss in the acceleration system. H^- ions are easily stripped by collisions with neutral molecules. The stripping loss of H^- ions within the extractor/accelerator structure is estimated as 16% at a source pressure of 0.7Pa. However, the ions are mostly stripped in the extraction gap. These electrons are trapped by the magnetic field and may not penetrate into the acceleration gap. The ratio of I_{acc}/H^- can not be explained only by the stripping during the acceleration gap. It is supposed that some of the neutrals stripped in the extraction gap have divergent trajectories and that they do strike the extraction grid and emitted secondary electrons contribute to I_{acc}. In the high energy beam acceleration of negative

ions it is very important to reduce the operating gas pressure not only for the reduction of the accelerated electrons but for the good beam optics.

B. Measurement of beam divergence angle of the H^- beams

The beam divergence angle is determined by the e-folding width of the spatial profiles measured by the calorimeter array. Figure 5(a) shows the dependence of the divergence angle on the acceleration voltage V_{acc}. Each curve corresponds to a different current density and an adequate V_{ext} is applied in order that the H^- current saturation due to the space charge limit does not occur. The optimum (minimum) divergent angle of 5mrad is obtained at each current density by adjusting V_{acc}. There is no effect on I_{acc} when V_{acc} changes as is shown in Fig.5(b). This indicates that I_{acc} is independent of the electric field in the acceleration gap and then of the beam trajectory during the gap.

Figure 6 shows a dependence of the beam divergence angle on the ratio of the electric field E_{acc} to E_{ext}, E_{acc}/E_{ext}. The optimum ratio for the minimum divergence is 1.6 and is almost the same value in all cases. Here, it is assumed that the extraction gap is 7mm, the thickness of the plasma grid of 2.5mm is added to d_{ext} of 4.5mm, and that the acceleration gap, d_{acc1}, is 40mm. It is remarkable that the dependency is almost the same in three different current densities.

A 2-D spatial profile of the H^- beam with the divergence angle of 5mrad and the current density of 15 mA/cm^2 is shown in Fig.7. The divergence angle of 5mrad is also obtained with the current density of 30 mA/cm^2. This figure is obtained by scanning the calorimeter array vertically. The profile is almost axi-symmetric. The peak position is moved slightly when V_{acc} is changed. This is the beam steering effect discussed later.

Figure 8(a) shows the dependence of the divergence angle on V_{acc} for three different P_{arc}. The V_{ext} is kept at constant and each symbol corresponds to the data before, just before and after the H^- current saturation. As shown in the figure the optimum value of V_{acc} to obtain the minimum divergence angle is changed slightly as P_{arc} increases. In a low P_{arc} operation the emitted beams tend to converge and lower V_{acc} is good for the optimum optics. When P_{arc} increases, the extracted beams tend to diverge and higher V_{acc} is necessary for the optimum

optics. Figure 8(b) shows the dependence of I_{acc} on V_{acc}. In this space charge limited region, I_{acc} is larger than that in the plasma density limited region as discussed in the previous section. The increased I_{acc} can not be suppressed by changing V_{acc} as shown in Fig.8(b). This indicates that the increased I_{acc} is not caused by the phenomena in the acceleration gap. These data support that the diverged beams partially collide with the extraction grid and emitted secondary electrons are accelerated as mentioned above. It is worth noting that even if the current density changes from 15mA/cm^2 to 30mA/cm^2 the accelerated beam divergence angle can be kept below 7mrad when V_{acc} is set at 75kV. This is favorable for the large H^- ion source where the density of the plasma is not perfectly uniform.

C. Double-stage acceleration of the H^- beams

The beam divergence angles are also measured in the double-stage acceleration system and compared with that in the single-stage experiments. Here, d_{ext} ,d_{acc1} and d_{acc2} are set at 3.5mm, 20mm, and 40mm, respectively. In Fig.9 the beam divergence angles are plotted as a function of E_{acc1}/E_{ext} in two cases of V_{acc1}/V_{acc2}, 23kV/50kV and 27kV/60kV. Here, it is assumed that the extraction gap is 6mm, the thickness of the plasma grid of 2.5mm is added to d_{ext} of 3.5mm. There is a optimum value of E_{acc1}/E_{ext} and is about 1.5, which is almost the same as the optimum ratio of V_{acc}/V_{ext} in the single-stage acceleration. The optimum value of the ratio is not changed when the current density changes from 15 to 30mA/cm^2.

A divergence angle is also affected by a second acceleration voltage V_{acc2}. Fig.10 shows the dependence of the divergence angle on V_{acc2} for several E_{acc1}/E_{ext}. A beam diverged by unmatched ratio of E_{acc1}/E_{ext} can be re-focused by changing V_{acc2}. It is noted that when V_{acc1} is set at optimum value for V_{ext}, the divergence angle is not affected by V_{acc2}. As is shown in the figure, a minimum divergence of 5mrad is also obtained in the double-stage acceleration system.

D. Beam steering by the permanent magnets

The H^- beams are extracted from 9 holes of 13mm in diameter. Measured spatial profiles is shown in Fig.11. Though the profile is somewhat distorted, there appear 9 peaks as is

shown in the figure. It is worth noting that each vertical raw of 3 peaks shifts up and downward. The shift of the beam position is caused by the steering effect by the permanent magnets buried in the extraction grid. A single particle trajectory in the electrodes is calculated with an assumed linear electric field and a measured magnetic field as is shown in Fig.12. The simple calculation indicates a beam steering angle is 8mrad in this experimental condition. Figure 13 shows calculated spatial profiles of the beam at 2m apart from the ion source, where the calorimeter is placed. Here, a beam divergence angle is assumed to be 6mrad and including the steering effect. The result is in good agreement with the measured profiles. The steering direction also agrees with the calculated one.

The steering angle is affected not only by the magnetic field but by the beam acceleration voltage. If the acceleration electric field is strong, a particle velocity increases and the beam steering angle decreases. It is observed in the single beamlet experiment that the beam's peak position shifts as the V_{acc} changes. The shifts of the beam are plotted as a function of V_{acc} in Fig.14. The dotted line in the figure corresponds to the calculated value of the shift and matches the observed dependence.

A beam steering by the bar-type magnetic filter is also observed. This shift, however, is unidirectional in all beamlets and the total beam direction can be modified by changing the ion source direction. In order to focus the beams from multi-beamlets at one point, the aperture displacement method can be utilized and it is necessary to consider this steering effect by the permanent magnets.

Acknowledgments

Authors would like to acknowledge to Dr. T.Okuyama, and Mr. Y.Suzuki for their help during the experiments.

References

a) present address : Department of Electrical Engineering, Faculty of Engineering, Tohoku University, Aoba, Sendai, 980-77, Japan.

1. T.Nagashima, R.S.Hemsworth, M.Makowski, D.Remsen, and the ITER Joint Central Team and Home Teams, Proceedings of the 15th International Conference on Plasma Physics and Controlled Nuclear Fusion Research, Seville, Spain, 1994, IAEA-CN-60 / E-P-9.
2. T.Inoue, M.Araki, M.Hanada, T.Kurashima, S.Matsuda, Y.Matsuda, Y.Ohara, Y.Okumura, S.Tanaka, and K.Watanabe, Nucl. Instr. Meth. **B37/38**, 111 (1989).
3. A.Ando, Y.Takeiri, K.Tsumori, O.Kaneko, Y.Oka, R.Akiyama, T.Kawamoto, K.Mineo, T.Kurata, and T.Kuroda, Rev. Sci. Instrum. **63**, 2683 (1992).
4. M.Hanada, T.Inoue, H.Kojima, Y.Matsuda, Y.Ohara, Y.Okumura, K.Watanabe, and M.Seki, *ibid.* **61**, 499 (1987).
5. S.R.Walther, K.N.Leung and W.B.Kunkel, J.Appl.Phys. **64**, 3424 (1988).
6. K.N.Leung, C.A.Hauck, W.B.Kunkel, and S.R.Walther, Rev. Sci. Instrum. **60**, 531(1989).
7. Y.Mori, T.Okuyama, A.Takagi, and D.Yuan, Nucl. Instr. and Meth. **A301**, 1 (1991).
8. Y.Okumura, M.Hanada, T.Inoue, H.Kojima, Y.Matsuda, Y.Ohara, M.Seki, and K.Watanabe, Proceedings of the 5th International Symposium on Production and Neutralization of Negative Ions and Beams, Brookhaven, 1989, (American Institute of Physics(AIP)-Conference proceedings No.210, Woodbury, NY, 1990), p.169.
9. Y.Okumura, M.Hanada, T.Inoue, H.Kojima, Y.Matsuda, Y.Ohara, Y.Oohara, M.Seki, Y.Suzuki and K.Watanabe, Proceedings of the 16th Symposium on Fusion Technology, 1990, London, (Elsevier Science Publishers, Amsterdam, 1991), p.1026.
10. A.Ando, K.Tsumori, Y.Takeiri, O.Kaneko, Y.Oka, T.Okuyama, H.Kojima, Y.Yamashita, R.Akiyama, T.Kawamoto, K.Mineo, T.Kurata and T.Kuroda, Proceedings of the 6th International Symposium on Production and Neutralization of

Negative Ions and Beams, 1992, Brookhaven, (American Institute of Physics(AIP)-Conference proceedings No.287, Woodbury, NY, 1994), p.339.

11. K.Tsumori, A.Ando, T.Okuyama, Y.Suzuki, O.Kaneko, Y.Oka, Y.Takeiri, R.Akiyama, T.Kawamoto, K.Seko and T.Kuroda, Fusion Engineering and Design. **26**, 473 (1995).

12. A.Iiyoshi, Proceedings of the 13th Symposium on Fusion Engineering, 1989, Knoxville, (the Institute of Electrical and Electronics Engineers, Inc. (IEEE), Piscataway, NJ, 1990), Vol.2, p.1007.

13. A.Ando, K.Tsumori, Y.Oka, O.Kaneko, Y.Takeiri, E.Asano, T.Kawamoto, R.Akiyama, and T.Kuroda, Phys Plasmas, **1**, 2813 (1994).

14. Y.Takeiri, A.Ando, O.Kaneko, Y.Oka, K.Tsumori, R.Akiyama, E.Asano, T.Kawamoto, T.Kuroda, M.Tanaka and H.Kawakami, to be published in Rev. Sci. Instrum. **66**, 2541 (1995).

15. Y.Takeiri, A.Ando, O.Kaneko, Y.Oka, K.Tsumori, R.Akiyama, E.Asano, T.Kawamoto, M.Tanaka and T.Kuroda, "High-Energy Acceleration of an Intense Negative Ion Beam", NIFS-report No.338.

16. T.Inoue, M.Hanada, M.Kuriyama, S.Maeno, M.Matsuoka, K.Miyamoto, Y.Ohara, Y.Okumura and K.Watanabe, Proceedings of the 15th International Conference on Plasma Physics and Controlled Nuclear Fusion Research, Seville, Spain, 1994, IAEA-CN-60/F-II-2.

17. T.Inoue, M.Hanada, M.Mizuno, Y.Ohara, Y.Okumura, Y.Suzuki, H.Tanaka, M.Tanaka and K.Watanabe, Proceedings of the IAEA Technical Committee Meeting on Negative Ion Based Neutral Beam Injectors, Naka, 1991, p.189-194.

Figure Captions

Fig. 1 Schematic diagram of the 1/3-scaled negative hydrogen ion source. The structure of the bar magnetic filter is described in the figure.

Fig. 2 Structures of (a) the single-stage and (b) the double-stage acceleration electrode system.

Fig. 3 Dependencies of (a) H^- current, (b) I_{acc} and (c) I_{acc}/H^- on P_{arc} for three different V_{ext} ; (open circles) V_{ext} = 9.3kV, (closed circles) V_{ext} =7.9kV, (crosses) V_{ext} = 6.6kV. V_{acc} = 50-80kV, p = 0.7Pa.

Fig. 4 (a) H^- current (open circles) and I_{acc} (closed circles), and (b) I_{acc}/H^- as a function of p. V_{ext} = 9.3kV, V_{acc} = 73kV, P_{arc} = 45-50kW .

Fig. 5 Dependence of (a) the beam divergence angle and (b) I_{acc} on V_{acc} at p = 0.7Pa for three different H^- current density ; (open circles) j^- = 15mA/cm^2, P_{arc} = 25kW, V_{ext}= 6.3kV; (closed circles) j^- = 22mA/cm^2, P_{arc} = 35kW, V_{ext}= 7.9kV; (crosses) j^- = 28mA/cm^2, P_{arc} = 45kW, V_{ext}= 9.3kV.

Fig. 6 Dependence of the beam divergence angle on E_{acc} / E_{ext}. Marks are the same as that in Fig.5.

Fig. 7 Two-dimensional profile of the H^- beam. P_{arc} = 36kW, V_{ext}= 7.9kV, V_{acc} = 73kV, j^- = 22mA/cm^2.

Fig. 8 Dependence of (a) the beam divergence angle and (b) I_{acc} on V_{acc} at p = 0.7Pa for three different P_{arc} ; (open circles) j^- = 15mA/cm^2, P_{arc} = 25kW, V_{ext}=

7.9kV; (closed circles) $j^- = 22mA/cm^2$, $P_{arc} = 35kW$, $V_{ext} = 7.9kV$; (crosses) $j^- = 22mA/cm^2$, $P_{arc} = 45kW$, $V_{ext} = 7.9kV$.

Fig. 9 The beam divergence angle as a function of E_{acc1}/E_{ext} in the double-stage acceleration. (open circles) $V_{acc1}/V_{acc2} = 23kV/50kV$, (closed circles) $V_{acc1}/V_{acc2} = 27kV/60kV$. $P_{arc} = 30kW$, $p = 0.9Pa$.

Fig.10 The beam divergence angle as a function of V_{acc2} in the double-stage acceleration. (open circles) $E_{acc1}/E_{ext} = 1.5$, (closed circles) $E_{acc1}/E_{ext} = 1.2$, (crosses) $E_{acc1}/E_{ext} = 0.9$, (open lozenge) $E_{acc1}/E_{ext} = 0.7$. $P_{arc} = 30kW$, $p = 0.9Pa$.

Fig.11 The measured (a) horizontal, (b) vertical and (c) two-dimensional spatial profiles of the H^- beams from nine beamlets. $V_{ext} = 7kV$, $V_{acc1}/V_{acc2} = 23kV/50kV$, $p = 1.2Pa$, $j^- = 8mA/cm^2$.

Fig.12 The calculated single particle trajectory. (a) a measured magnetic field strength, (b) a electric potential assumed in the calculation, (c) a calculated H- beam trajectory and (d) a beam steering angle as a function of the beam position.

Fig.13 The calculated (a) horizontal, (b) vertical and (c) two-dimensional spatial profiles of the H^- beams. It is assumed the steering angle is 8mrad and the beam divergence angle is 6mrad.

Fig.14 Beam steering angle as a function of V_{acc}. Open circles are obtained in the single-stage acceleration and dotted line corresponds to the calculation.

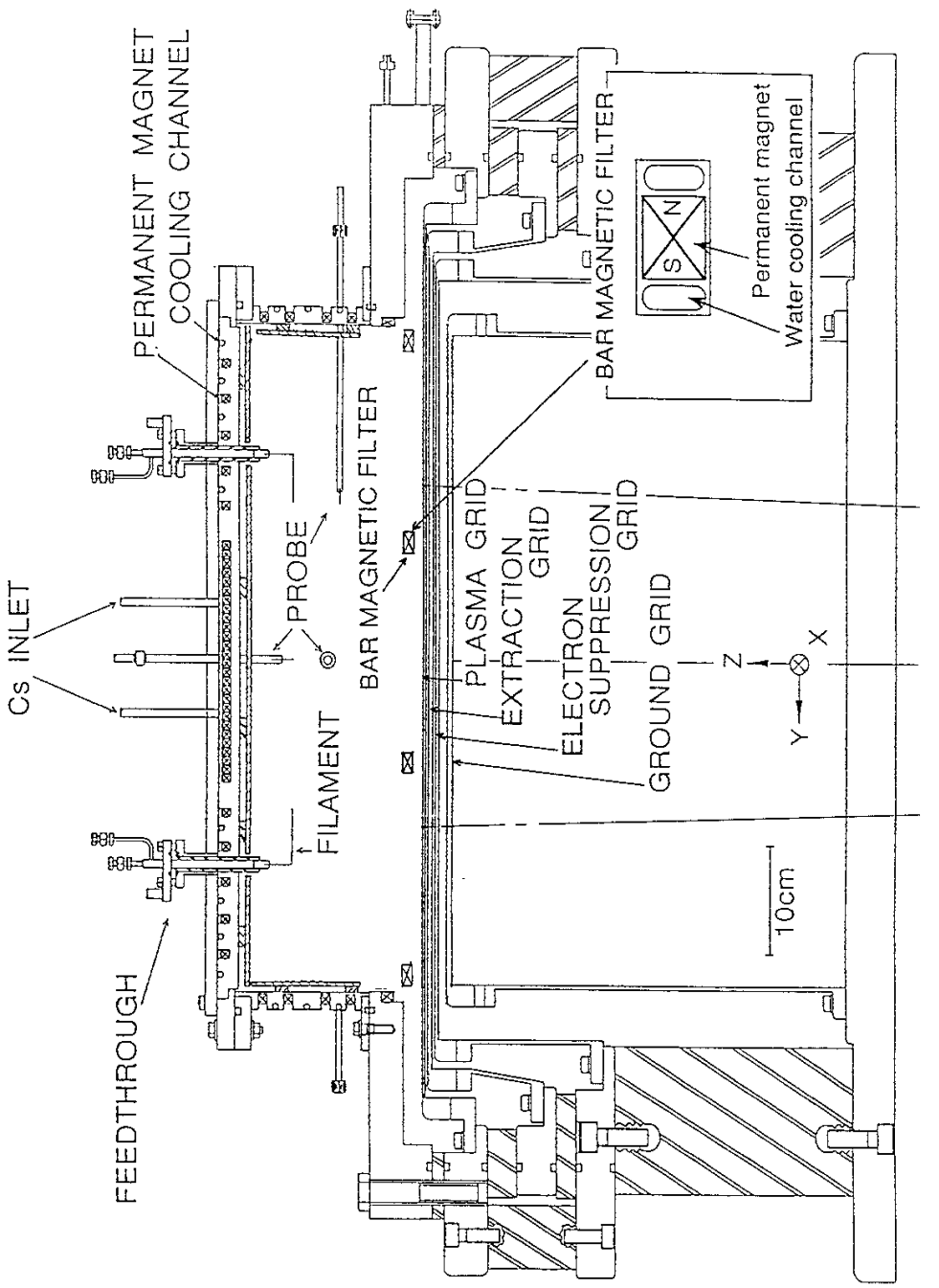
PERMANENT MAGNET
COOLING CHANNEL
Cs INLET
PROBE
BAR MAGNETIC FILTER
FILAMENT
FEEDTHROUGH
PLASMA GRID
EXTRACTION GRID
ELECTRON SUPPRESSION GRID
GROUND GRID
BAR MAGNETIC FILTER
Permanent magnet
Water cooling channel
S
N
Z
X
Y
10cm

Fig.1

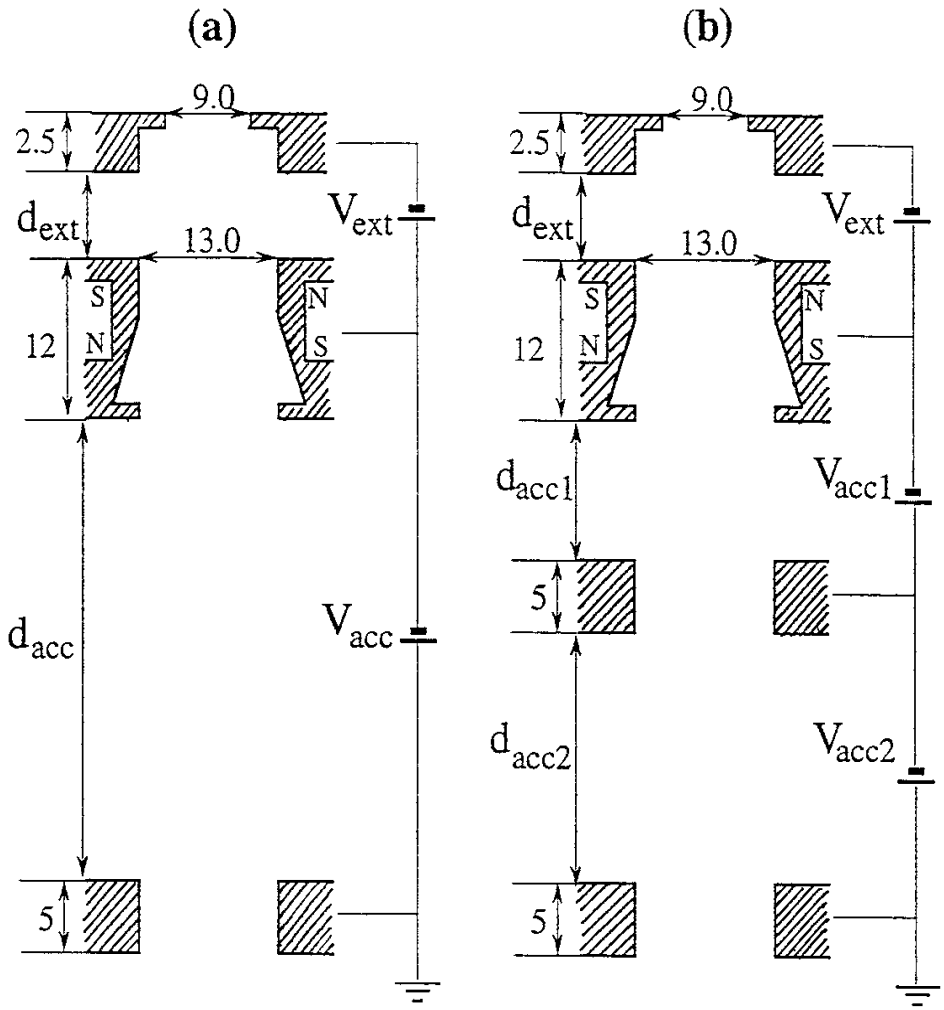
(a)
(b)
9.0
2.5
d_{ext}
13.0
12
S
N
N
S
V_{ext}
d_{acc}
V_{acc}
5
d_{acc1}
V_{acc1}
d_{acc2}
V_{acc2}

Fig.2

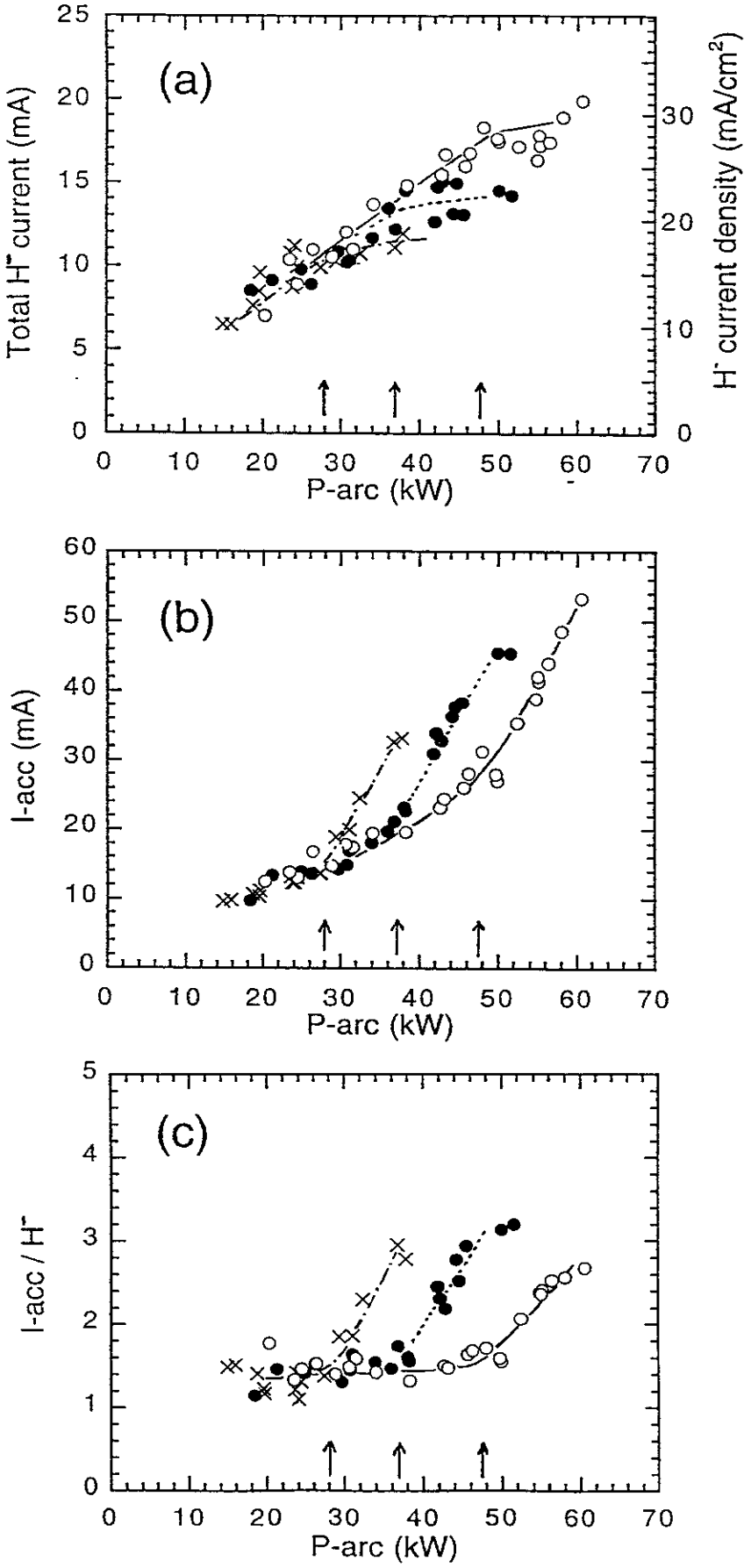
(a)
Total H⁻ current (mA)
H⁻ current density (mA/cm²)
P-arc (kW)
(b)
I-acc (mA)
P-arc (kW)
(c)
I-acc / H⁻
P-arc (kW)

Fig.3

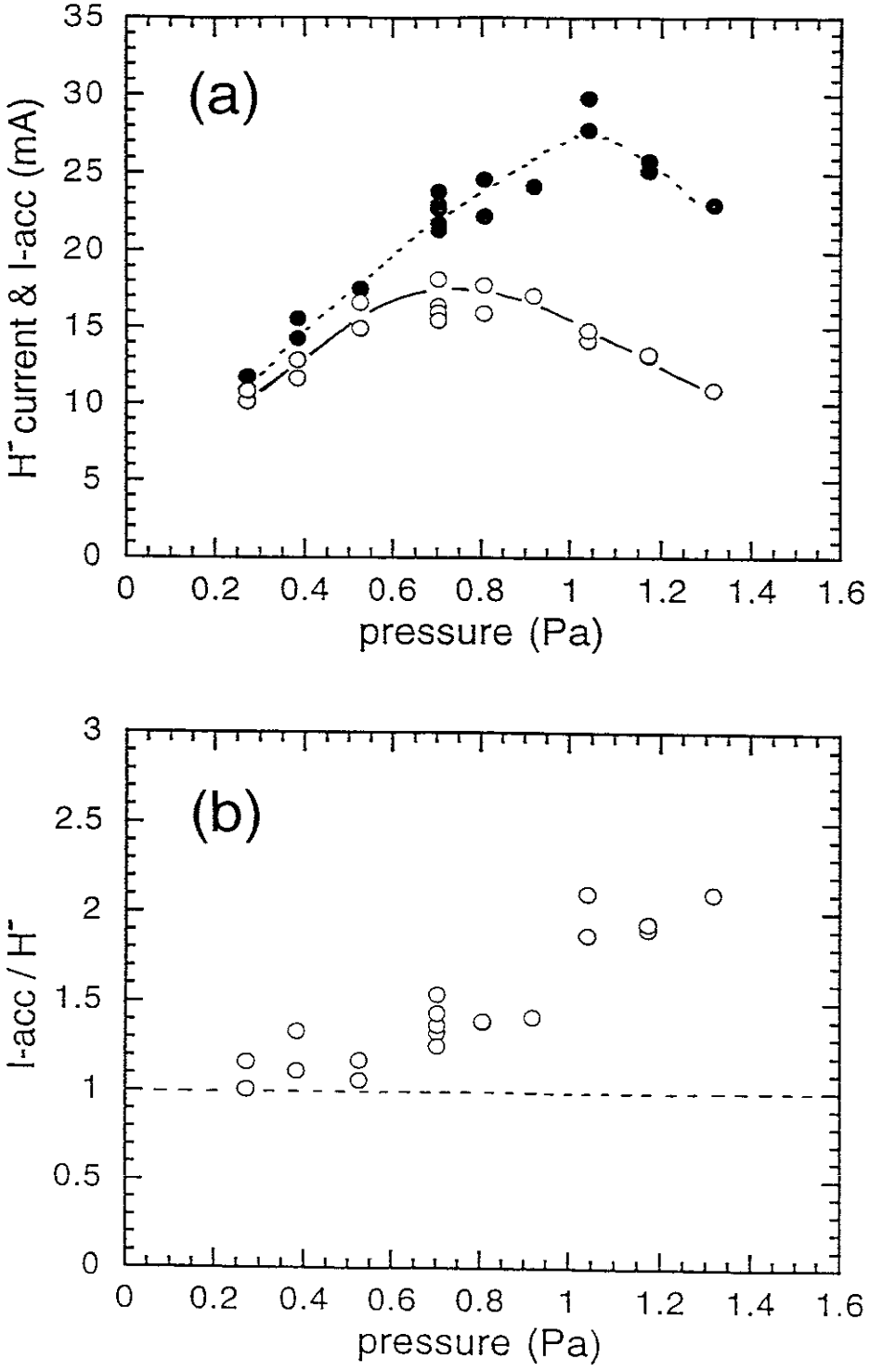

Fig.4

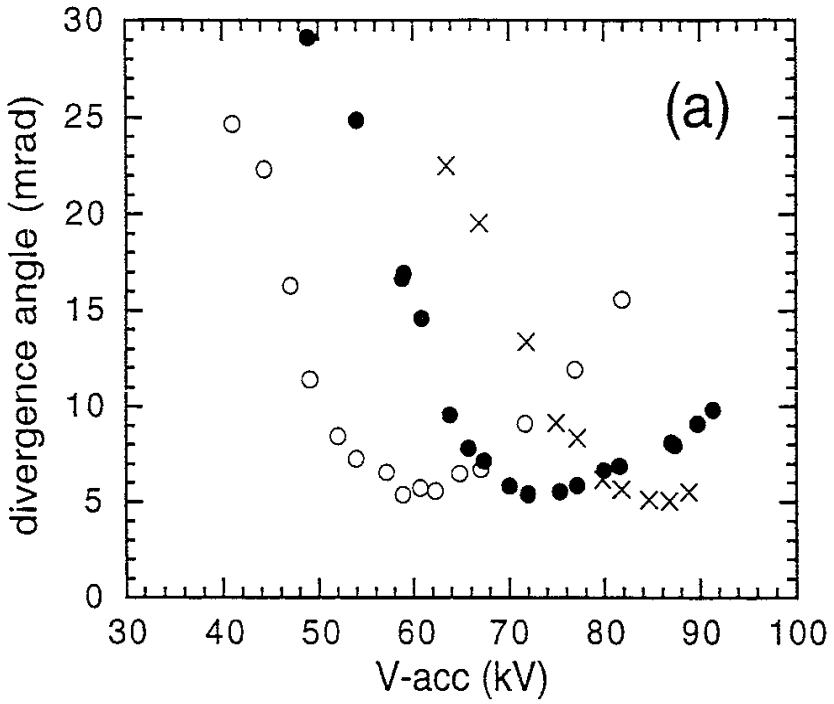
(a)
divergence angle (mrad)
V-acc (kV)
0
5
10
15
20
25
30
30
40
50
60
70
80
90
100

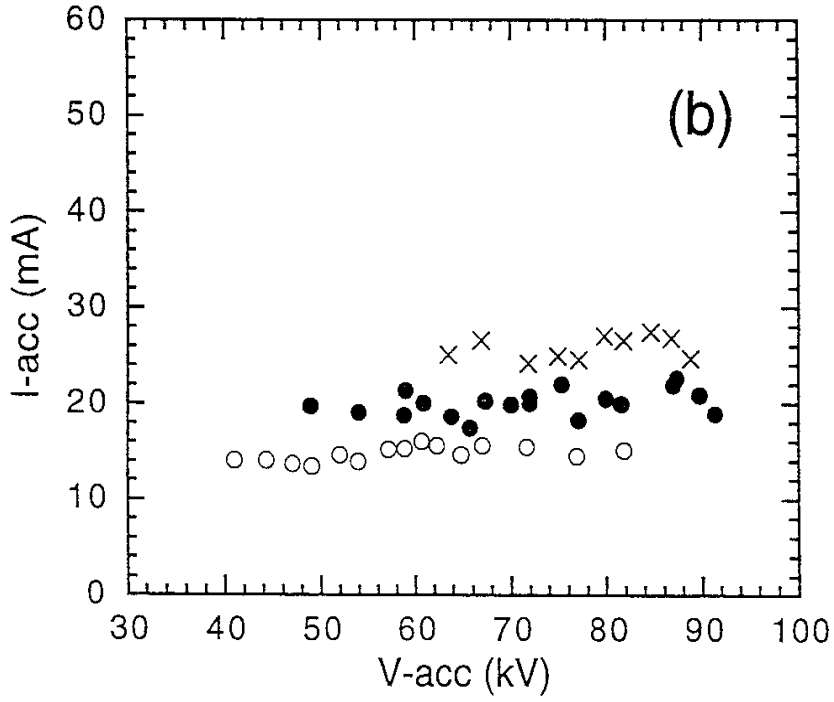
(b)
I-acc (mA)
V-acc (kV)
0
10
20
30
40
50
60
30
40
50
60
70
80
90
100

Fig.5

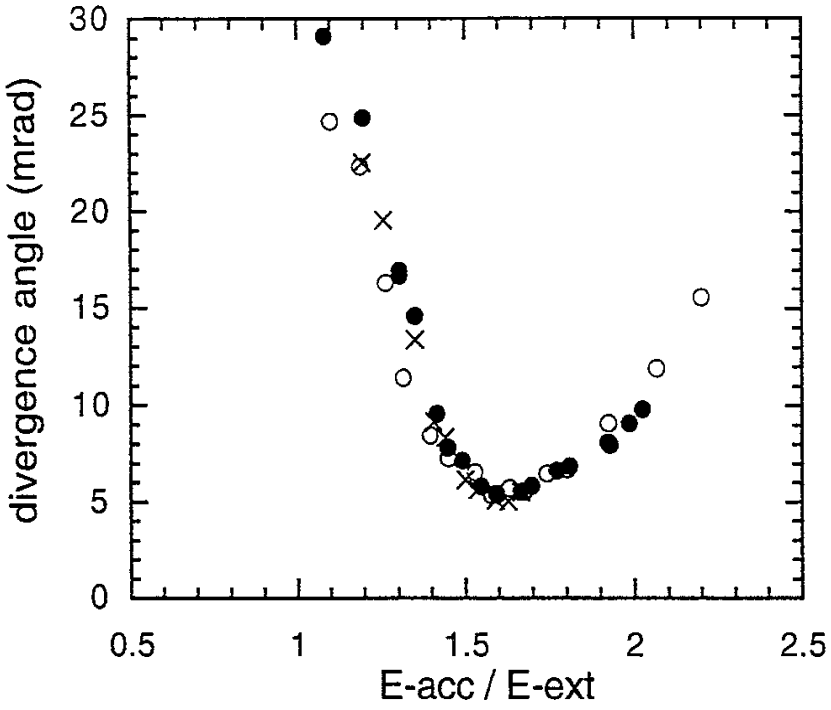

Fig.6

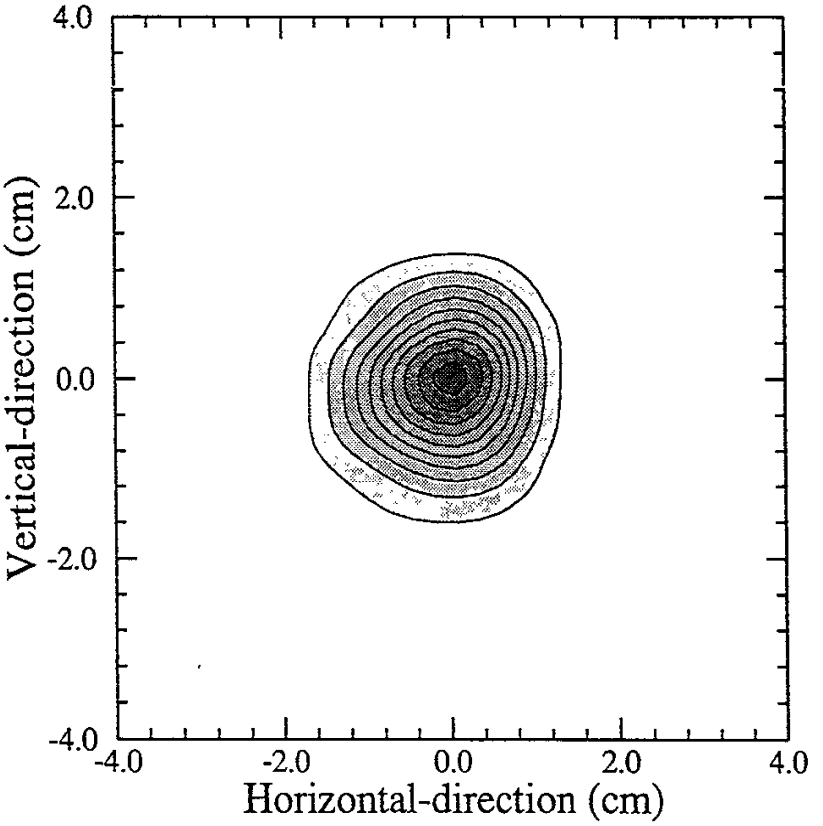
4.0
2.0
0.0
-2.0
-4.0
Vertical-direction (cm)
-4.0
-2.0
0.0
2.0
4.0
Horizontal-direction (cm)

Fig.7

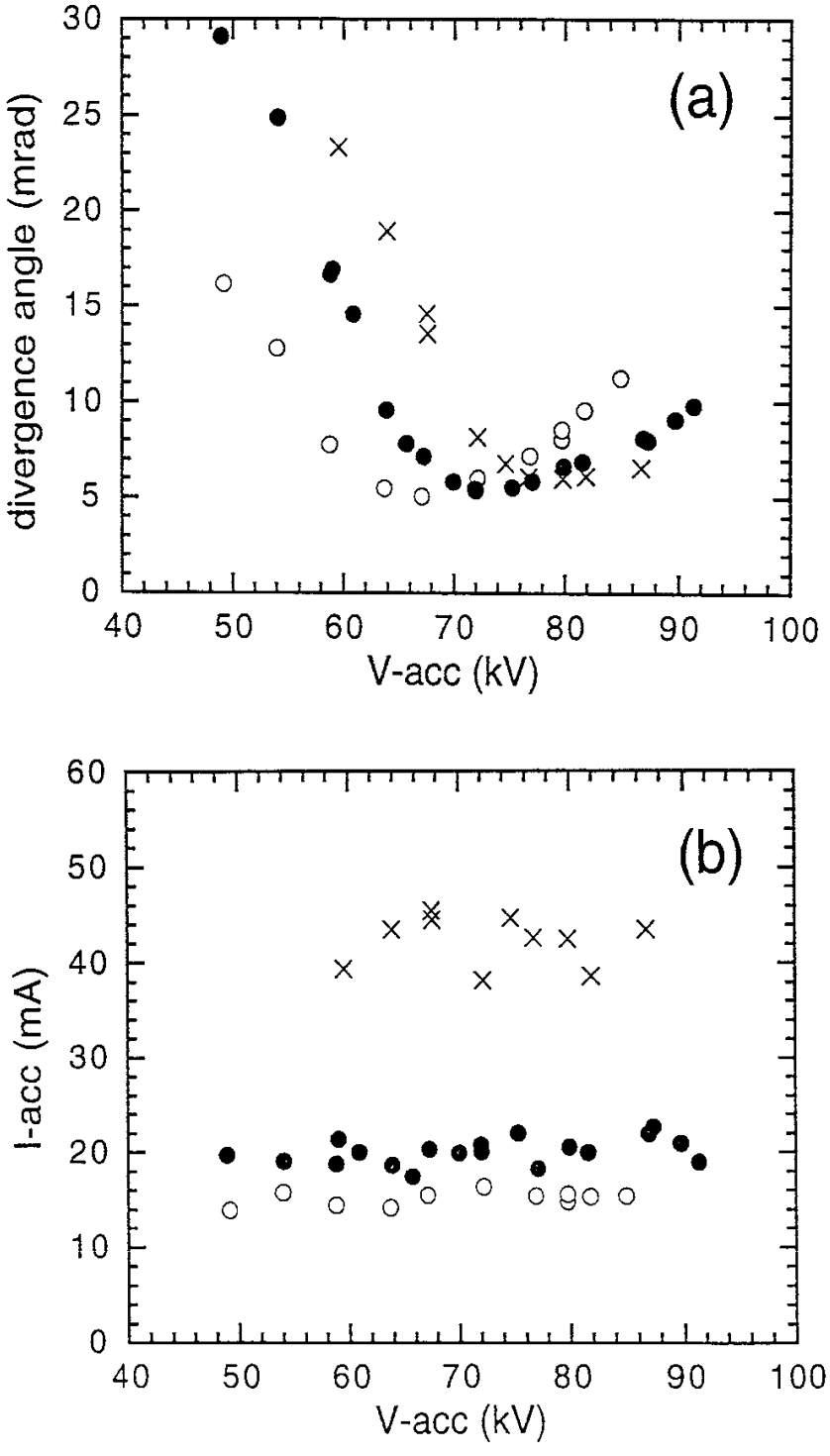

Fig.8

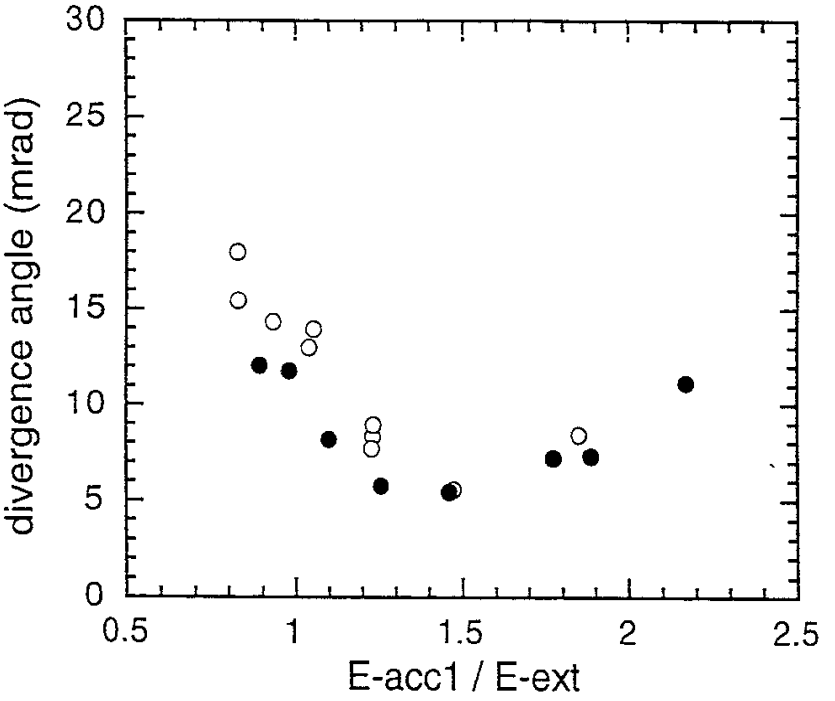

Fig.9

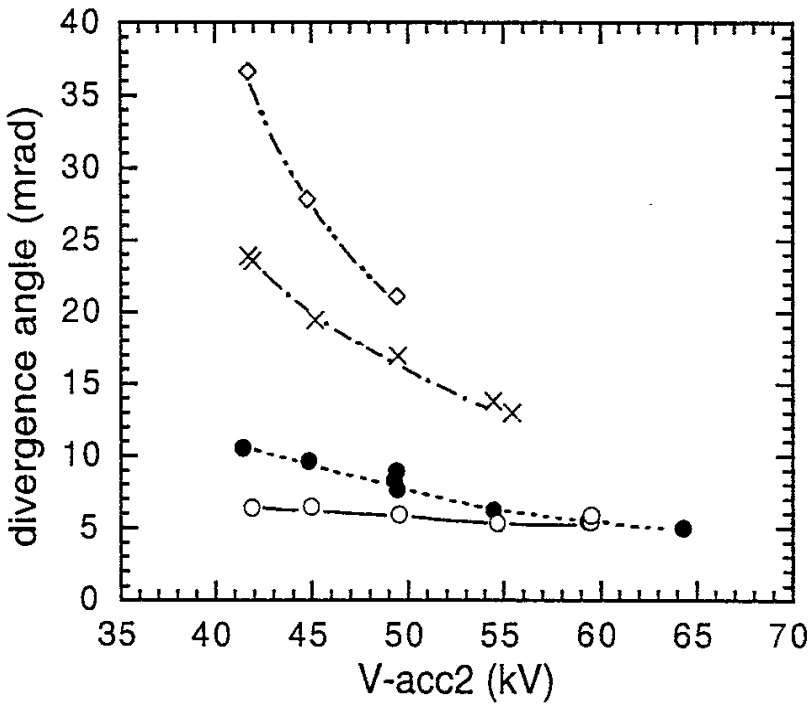
divergence angle (mrad)
40
35
30
25
20
15
10
5
0
35
40
45
50
55
60
65
70
V-acc2 (kV)

Fig.10

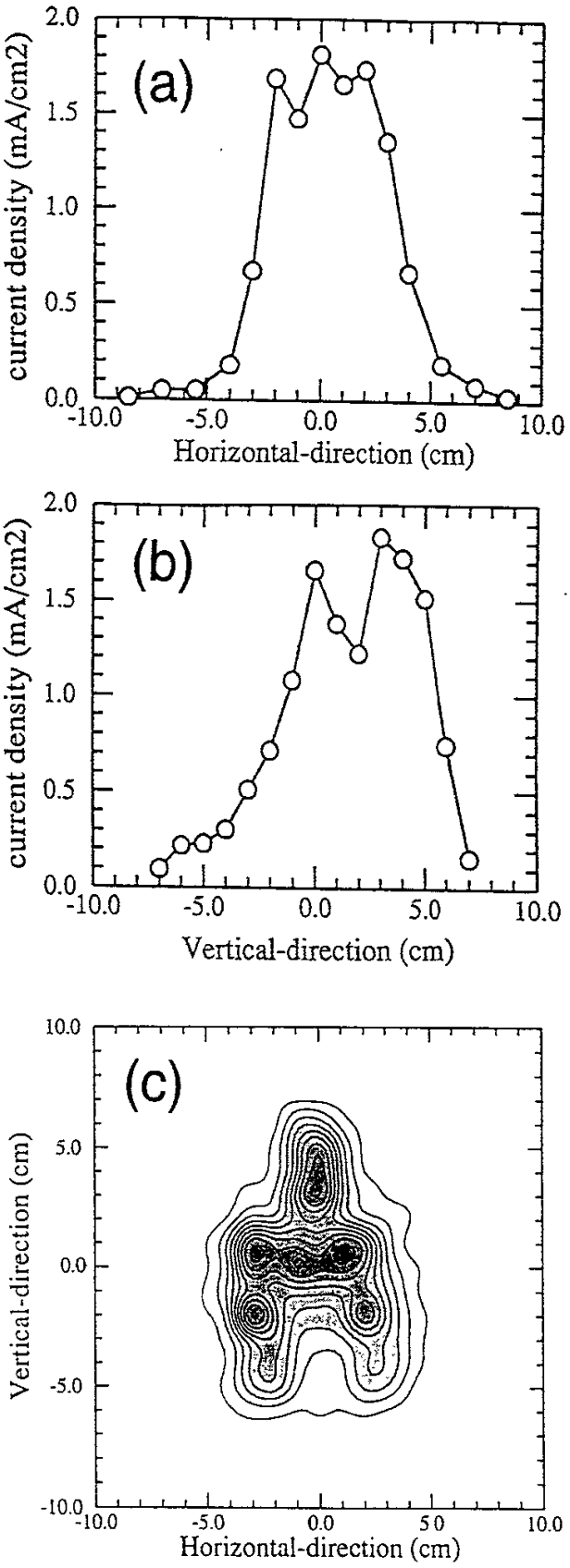
(a)
current density (mA/cm2)
2.0
1.5
1.0
0.5
0.0
-10.0
-5.0
0.0
5.0
10.0
Horizontal-direction (cm)
(b)
current density (mA/cm2)
Vertical-direction (cm)
(c)
Vertical-direction (cm)
10.0
5.0
0.0
-5.0
-10.0
Horizontal-direction (cm)

Fig.11

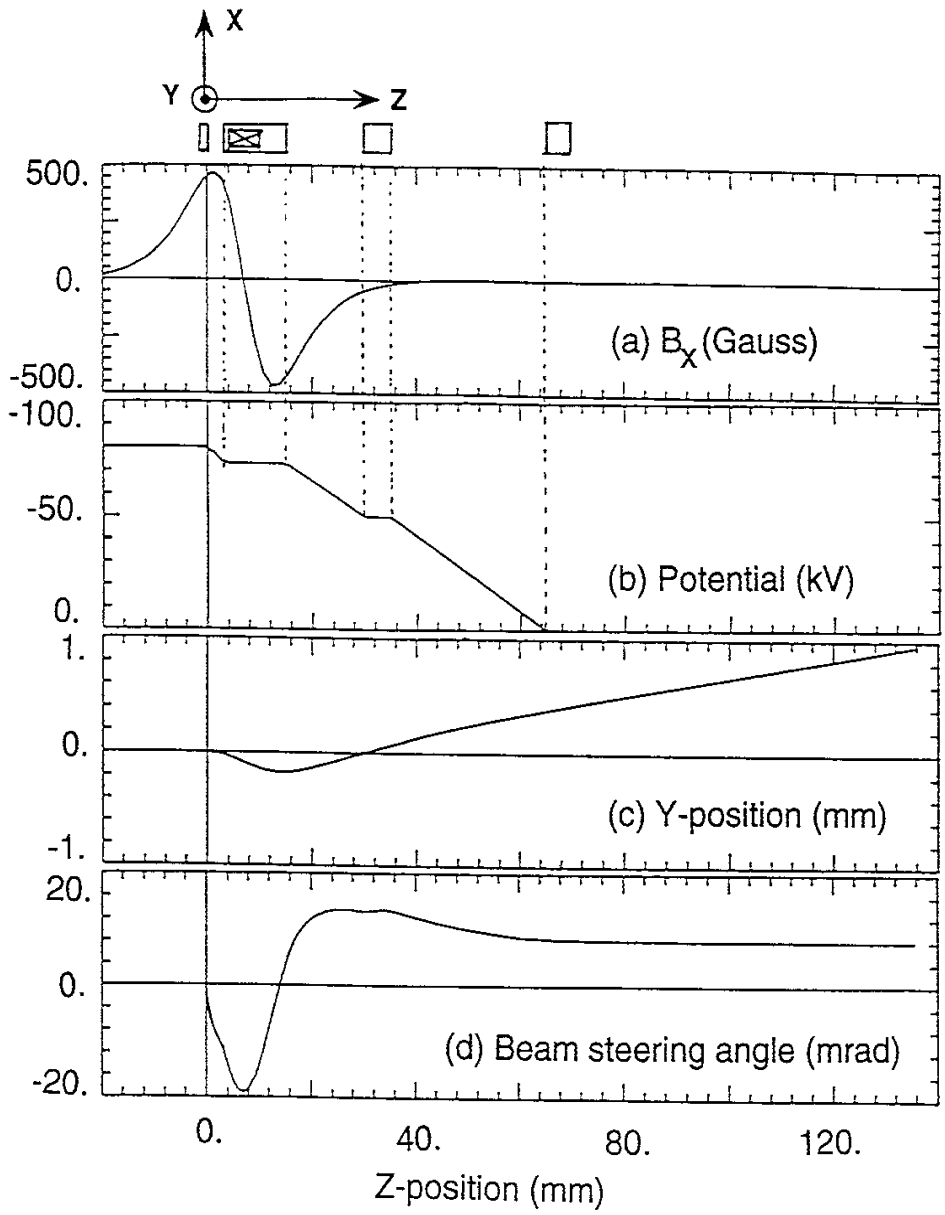
X
Y
Z
500.
0.
-500.
(a) B_X (Gauss)
-100.
-50.
0.
(b) Potential (kV)
1.
0.
-1.
(c) Y-position (mm)
20.
0.
-20.
(d) Beam steering angle (mrad)
0.
40.
80.
120.
Z-position (mm)

Fig.12

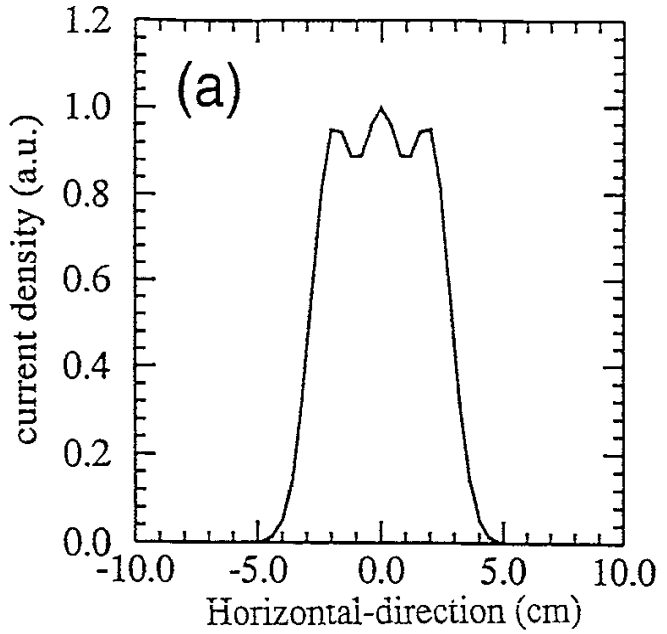
(a)
current density (a.u.)
1.2
1.0
0.8
0.6
0.4
0.2
0.0
-10.0
-5.0
0.0
5.0
10.0
Horizontal-direction (cm)

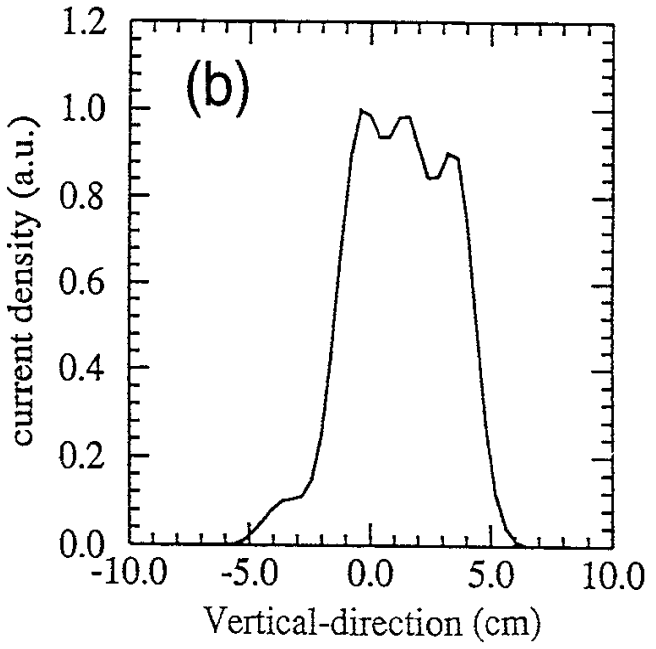
(b)
current density (a.u.)
1.2
1.0
0.8
0.6
0.4
0.2
0.0
-10.0
-5.0
0.0
5.0
10.0
Vertical-direction (cm)

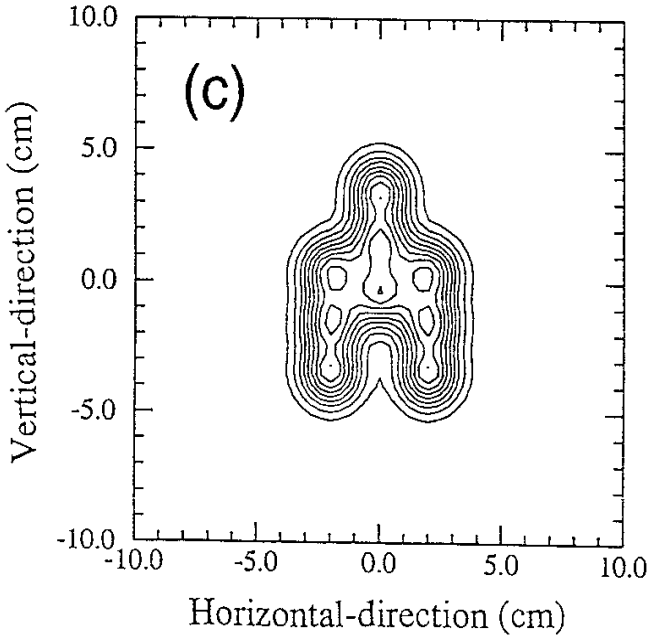
(c)
Vertical-direction (cm)
10.0
5.0
0.0
-5.0
-10.0
-10.0
-5.0
0.0
5.0
10.0
Horizontal-direction (cm)

Fig.13

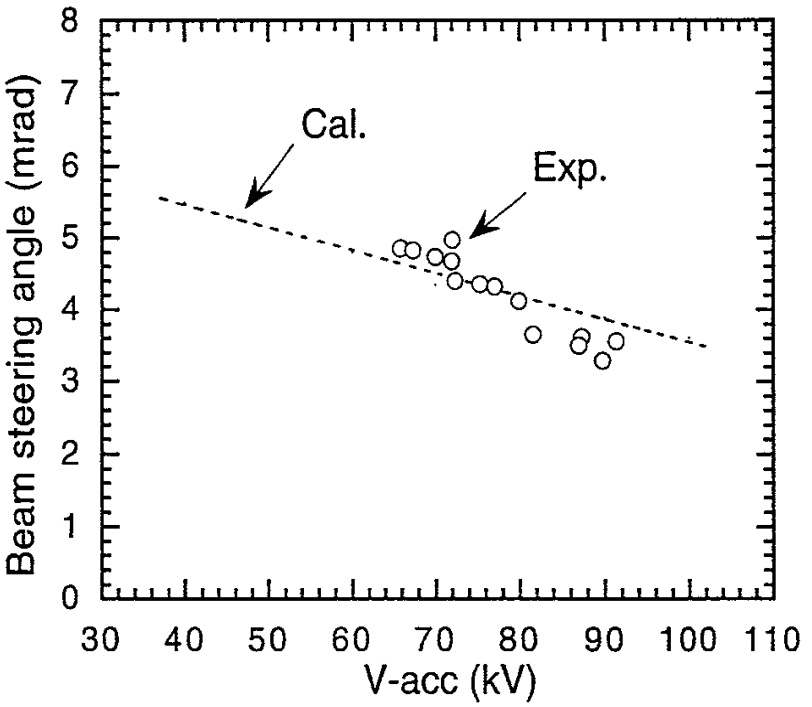
Beam steering angle (mrad)
8
7
6
5
4
3
2
1
0
Cal.
Exp.
30
40
50
60
70
80
90
100
110
V-acc (kV)

Fig.14

Recent Issues of NIFS Series

NIFS-320 A. Kageyama, T. Sato and The Complexity Simulation Group,
Computer Simulation of a Magnetohydrodynamic Dynamo II: Nov. 1994

NIFS-321 A. Bhattacharjee, T. Hayashi, C.C.Hegna, N. Nakajima and T. Sato,
Theory of Pressure-induced Islands and Self-healing in Three-dimensional Toroidal Magnetohydrodynamic Equilibria; Nov. 1994

NIFS-322 A. Iiyoshi, K. Yamazaki and the LHD Group,
Recent Studies of the Large Helical Device: Nov. 1994

NIFS-323 A. Iiyoshi and K. Yamazaki,
The Next Large Helical Devices; Nov. 1994

NIFS-324 V.D. Pustovitov
Quasisymmetry Equations for Conventional Stellarators; Nov. 1994

NIFS-325 A. Taniike, M. Sasao, Y. Hamada, J. Fujita, M. Wada,
The Energy Broadening Resulting from Electron Stripping Process of a Low Energy Au^- Beam; Dec. 1994

NIFS-326 I. Viniar and S. Sudo,
New Pellet Production and Acceleration Technologies for High Speed Pellet Injection System "HIPEL" in Large Helical Device; Dec. 1994

NIFS-327 Y. Hamada, A. Nishizawa, Y. Kawasumi, K. Kawahata, K. Itoh, A. Ejiri, K. Toi, K. Narihara, K. Sato, T. Seki, H. Iguchi, A. Fujisawa, K. Adachi, S. Hidekuma, S. Hirokura, K. Ida, M. Kojima, J. Koong, R. Kumazawa, H. Kuramoto, R. Liang, T. Minami, H. Sakakita, M. Sasao, K.N. Sato, T. Tsuzuki, J. Xu, I. Yamada, T. Watari,
Fast Potential Change in Sawteeth in JIPP T-IIU Tokamak Plasmas; Dec. 1994

NIFS-328 V.D. Pustovitov,
Effect of Satellite Helical Harmonics on the Stellarator Configuration; Dec. 1994

NIFS-329 K. Itoh, S-I. Itoh and A. Fukuyama,
A Model of Sawtooth Based on the Transport Catastrophe; Dec. 1994

NIFS-330 K. Nagasaki, A. Ejiri,
Launching Conditions for Electron Cyclotron Heating in a Sheared Magnetic Field; Jan. 1995

NIFS-331 T.H. Watanabe, Y. Todo, R. Horiuchi, K. Watanabe, T. Sato,
An Advanced Electrostatic Particle Simulation Algorithm for Implicit Time Integration: Jan. 1995

NIFS-332 N. Bekki and T. Karakisawa,
Bifurcations from Periodic Solution in a Simplified Model of Two-dimensional Magnetoconvection; Jan. 1995

NIFS-333 K. Itoh, S.-I. Itoh, M. Yagi, A. Fukuyama,
Theory of Anomalous Transport in Reverse Field Pinch; Jan. 1995

NIFS-334 K. Nagasaki, A. Isayama and A. Ejiri
Application of Grating Polarizer to 106.4GHz ECH System on Heliotron-E; Jan. 1995

NIFS-335 H. Takamaru, T Sato, R. Horiuchi, K. Watanabe and Complexity Simulation Group,
A Self-Consistent Open Boundary Model for Particle Simulation in Plasmas; Feb. 1995

NIFS-336 B.B. Kadomtsev,
Quantum Telegragh : is it possible?; Feb. 1995

NIFS-337 B.B.Kadomtsev,
Ball Lightning as Self-Organization Phenomenon; Feb. 1995

NIFS-338 Y. Takeiri, A. Ando, O. Kaneko, Y. Oka, K. Tsumori, R. Akiyama, E. Asano, T. Kawamoto, M. Tanaka and T. Kuroda,
High-Energy Acceleration of an Intense Negative Ion Beam; Feb. 1995

NIFS-339 K. Toi, T. Morisaki, S. Sakakibara, S. Ohdachi, T.Minami, S. Morita, H. Yamada, K. Tanaka, K. Ida, S. Okamura, A. Ejiri, H. Iguchi, K. Nishimura, K. Matsuoka, A. Ando, J. Xu, I. Yamada, K. Narihara, R. Akiyama, H. Idei, S. Kubo, T. Ozaki, C. Takahashi, K. Tsumori,
H-Mode Study in CHS; Feb. 1995

NIFS-340 T. Okada and H. Tazawa,
Filamentation Instability in a Light Ion Beam-plasma System with External Magnetic Field; Feb. 1995

NIFS-341 T. Watanbe, G. Gnudi,
A New Algorithm for Differential-Algebraic Equations Based on HIDM; Feb. 13, 1995

NIFS-342 Y. Nejoh,
New Stationary Solutions of the Nonlinear Drift Wave Equation; Feb. 1995

NIFS-343 A. Ejiri, S. Sakakibara and K. Kawahata,
Signal Based Mixing Analysis for the Magnetohydrodynamic Mode Reconstruction from Homodyne Microwave Reflectometry; Mar.. 1995

NIFS-344 B.B.Kadomtsev, K. Itoh, S.-I. Itoh

Fast Change in Core Transport after L-H Transition; Mar. 1995

NIFS-345 W.X. Wang, M. Okamoto, N. Nakajima and S. Murakami,
An Accurate Nonlinear Monte Carlo Collision Operator; Mar. 1995

NIFS-346 S. Sasaki, S. Takamura, S. Masuzaki, S. Watanabe, T. Kato, K. Kadota,
Helium I Line Intensity Ratios in a Plasma for the Diagnostics of Fusion Edge Plasmas; Mar. 1995

NIFS-347 M. Osakabe,
Measurement of Neutron Energy on D-T Fusion Plasma Experiments; Apr. 1995

NIFS-348 M. Sita Janaki, M.R. Gupta and Brahmananda Dasgupta,
Adiabatic Electron Acceleration in a Cnoidal Wave; Apr. 1995

NIFS-349 J. Xu, K. Ida and J. Fujita,
A Note for Pitch Angle Measurement of Magnetic Field in a Toroidal Plasma Using Motional Stark Effect; Apr. 1995

NIFS-350 J. Uramoto,
Characteristics for Metal Plate Penetration of a Low Energy Negative Muonlike or Pionlike Particle Beam: Apr. 1995

NIFS-351 J. Uramoto,
An Estimation of Life Time for A Low Energy Negative Pionlike Particle Beam: Apr. 1995

NIFS-352 A. Taniike,
Energy Loss Mechanism of a Gold Ion Beam on a Tandem Acceleration System: May 1995

NIFS-353 A. Nishizawa, Y. Hamada, Y. Kawasumi and H. Iguchi,
Increase of Lifetime of Thallium Zeolite Ion Source for Single-Ended Accelerator: May 1995

NIFS-354 S. Murakami, N. Nakajima, S. Okamura and M. Okamoto,
Orbital Aspects of Reachable β Value in NBI Heated Heliotron/Torsatrons; May 1995

NIFS-355 H. Sugama and W. Horton,
Neoclassical and Anomalous Transport in Axisymmetric Toroidal Plasmas with Electrostatic Turbulence; May 1995

NIFS-356 N. Ohyabu
A New Boundary Control Scheme for Simultaneous Achievement of H-mode and Radiative Cooling (SHC Boundary); May 1995

NIFS-357 Y. Hamada, K.N. Sato, H. Sakakita, A. Nishizawa, Y. Kawasumi, R. Liang,

K. Kawahata, A. Ejiri, K. Toi, K. Narihara, K. Sato, T. Seki, H. Iguchi, A. Fujisawa, K. Adachi, S. Hidekuma, S. Hirokura, K. Ida, M. Kojima, J. Koong, R. Kumazawa, H. Kuramoto, T. Minami,. M. Sasao, T. Tsuzuki, J.Xu, I. Yamada, and T. Watari,
Large Potential Change Induced by Pellet Injection in JIPP T-IIU Tokamak Plasmas; May 1995

NIFS-358 M. Ida and T. Yabe,
Implicit CIP (Cubic-Interpolated Propagation) Method in One Dimension; May 1995

NIFS-359 A. Kageyama, T. Sato and The Complexity Simulation Group,
Computer Has Solved A Historical Puzzle: Generation of Earth's Dipole Field; June 1995

NIFS-360 K. Itoh, S.-I. Itoh, M. Yagi and A. Fukuyama,
Dynamic Structure in Self-Sustained Turbulence; June 1995

NIFS-361 K. Kamada, H. Kinoshita and H. Takahashi,
Anomalous Heat Evolution of Deuteron Implanted Al on Electron Bombardment; June 1995

NIFS-362 V.D. Pustovitov,
Suppression of Pfirsch-schlüter Current by Vertical Magnetic Field in Stellarators; June 1995

NIFS-363 A. Ida, H. Sanuki and J. Todoroki
An Extended K-dV Equation for Nonlinear Magnetosonic Wave in a Multi-Ion Plasma; June 1995

NIFS-364 H. Sugama and W. Horton
Entropy Production and Onsager Symmetry in Neoclassical Transport Processes of Toroidal Plasmas; July 1995

NIFS-365 K. Itoh, S.-I. Itoh, A. Fukuyama and M. Yagi,
On the Minimum Circulating Power of Steady State Tokamaks; July 1995

NIFS-366 K. Itoh and Sanae-I. Itoh,
The Role of Electric Field in Confinement; July 1995

NIFS-367 F. Xiao and T. Yabe
A Rational Function Based Scheme for Solving Advection Equation; July 1995

NIFS-368 Y. Takeiri, O. Kaneko, Y. Oka, K. Tsumori, E. Asano, R. Akiyama, T. Kawamoto and T. Kuroda,
Multi-Beamlet Focusing of Intense Negative Ion Beams by Aperture Displacement Technique; Aug. 1995